Amphiphilic Graft Copolymer in a Selective Solvent: Intramolecular Structures and Conformational Transitions

O. V. Borisov* and E. B. Zhulina

Institute of Macromolecular Compounds of the Russian Academy of Sciences, 199004, St. Petersburg, Russia, and DRFMC/SI3M, CEA-Grenoble, 38000 Grenoble, France

Received December 9, 2004; Revised Manuscript Received January 19, 2005

ABSTRACT: We present a scaling theory for the equilibrium conformations of amphiphilic comblike (graft-) copolymer in dilute solution. We examine intramolecular self-assembly upon inferior solvent strength for the backbone. We demonstrate that at sufficiently dense grafting the backbone collapses via formation of a pearl necklace of intrachain micelles that are stabilized by steric repulsion between coronas. This behavior is reminiscent to the Rayleigh instability in hydrophobic polyelectrolyte, though occurs in a neutral macromolecule. The equilibrium local structure and the persistence length of comblike copolymer are analyzed as a function of solvent strength. Repulsion between micellar coronas leads to swelling of comblike macromolecule on larger scales and ensures the thermodynamic stability of the solution with respect to phase separation. In the case of sparse grafting we predict formation of not only spherical but also cylindrical intramolecular micelles and lamellar mesophases.

1. Introduction

Amphiphilic copolymers are capable to self-assembly into nanoscale superstructures in solutions, in the bulk phase, and at interfaces. A typical example is a diblock copolymer in selective solvent that gives rise to micelles in dilute solutions and mesophases of various morphologies in concentrated solutions.[1] Advanced synthetic approaches (such as controlled/living radical polymerization, "grafting to" and "grafting from" techniques, etc.) produce amphiphilic copolymers of various well-defined architectures (multiblock, star- and comblike, dendrimers, etc.).[2,3] Self-assembly in such copolymers is determined not only by the intramolecular lyophilic/lyophobic balance but also by the polymer topology. In particular, not only intermolecular but also intramolecular aggregation is possible.

Comblike amphiphilic copolymer with chemically different backbone and side chains has a number of features that make it an attractive candidate for diverse applications (delivery and release of drugs, agrochemistry, personal care and food products, etc.). Depending on solubility of the main chain and of the side chains, two qualitatively different scenarios of aggregation behavior are visible.

Under poor solvent conditions for side chains, the grafts "work" as "stickers". The attraction between the grafts leads to collapse of individual polymer molecule and macro phase separation in the solution. Such behavior is typical for the so-called polysoaps with sparsely grafted short side chains.[4] A qualitatively different scenario is expected for comblike copolymer with soluble side chains and collapsing backbone. We demonstrate below that such a copolymer can form the so-called pearl necklace of intramolecular micelles. The necklaces are stabilized against aggregation by repulsion between the side chains, and the solution remains homogeneous.

The conformations of comblike polymers in good solvents and those of polysoaps have been studied in the literature. A theory for nonionic comblike polymer in a good (or Θ) nonselective solvent was developed in refs 5−9. It was demonstrated that conformations of strongly branched (densely grafted) comblike polymers are characterized by significant extension of both the side chains and the backbone. This extension leads to reduction in the number of unfavorable monomer−monomer contacts arising due to high local intramolecular polymer concentration imposed by the branched topology. To the best of our knowledge, the conformations of comblike copolymer with collapsing backbone have not been considered previously.

The aim of the present paper is to study conformations of comblike copolymer upon inferior solvent strength for the main chain while the solvent remains good for the side chains. We examine the equilibrium structure of such comblike copolymer as a function of architectural parameters (degrees of polymerization of the side chains and the grafting density) and of the solvent strength for the backbone. We demonstrate that the conformations of comblike molecule and the thermodynamic stability of copolymer solution are governed by relative dimensions of the side chain and of the spacer. The rest of the paper is organized as follows. The theoretical model is described in section 2. In section 3, we consider the conformations of molecular bottle-brush (densely grafted comblike copolymer). We analyze here the longitudinal instability developing under inferior solvent strength and its effect on the large scale conformation of copolymer molecule. In section 4, we consider the case of sparsely grafted comblike polymer and analyze the morphological transitions between intramolecular micelles. In section 5, we discuss the scaling diagram of states for dilute copolymer solution. The conclusions are summarized in section 6.

2. Model of Comblike Polymer

We consider a comblike copolymer with side chains of degree of polymerization n grafted at one end onto the main chain (backbone) of total degree of polymerization M, Figure 1.

The number of monomers in the segment of the backbone separating two neighboring grafting points (the spacer) is $(m - 1)$. The number of grafts in the

* To whom correspondence should be addressed at CEA-Grenoble.

10.1021/ma047464s CCC: $30.25
Published on Web 02/25/2005

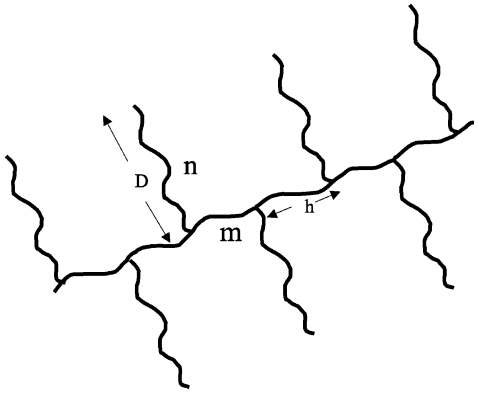

Figure 1. Comblike copolymer. n is the degree of polymerization of a side chain, m is the degree of polymerization of a spacer.

macromolecule is M/m, and the total degree of polymerization is $M + N$ where $N = nM/m$ is the total number of monomers in the side chains. We assume that the number of grafts is sufficiently large, $M/m \gg 1$, and neglect the effects arising from finite length of the main chain. We also assume that both the spacers and the grafted chains are intrinsically flexible. That is, the statistical segment length is the same for the side chains and for the main chain, and is on the order of monomer length a. (Below we use a as the unit length.)

The monomer−monomer interactions (solvent quality) are described by dimensionless second, v_m, v_n and third, $w_m \simeq w_n \simeq 1$, virial coefficients for monomers of the main and of the side chains, respectively. These virial coefficients are respectively normalized by the factors a^{-3} and a^{-6}. We assume that the solvent is good for the side chains, $v_n \equiv v \lesssim 1$. The solvent strength for the backbone can be tuned (e.g., by variations in temperature) from Θ to poor solvent conditions, $v_m \cong -\tau \leq 0$, where $\tau = (T - \theta)/\theta$ and θ is the Θ temperature for the backbone. (The case when solvent is equally good for the backbone and for the side chain was considered previously in ref 5.) We note that due to the different chemical natures of the monomers of the main chain and those of the side chains, the cross-interactions effectively reduce the solvent strength for the solvophobic backbone. The quantitative analysis of the related effects goes, however, beyond the scope of our analysis.

The degree of branching of the comblike copolymer is specified by the ratio

$$\gamma \cong \frac{n^{3/5}v^{1/5}}{m^{1/2}} \tag{1}$$

where $n^{3/5}v^{1/5}$ is the size of an individual side chain in a good solvent, and $m^{1/2}$ is the size of a spacer under Θ solvent conditions. For dense grafting, $\gamma \gg 1$, the neighboring side chains are considerably overlapped. Therefore, the local structure of the macromolecule (i.e., the conformations of both spacers and side chains) is strongly affected by the interactions between the side chains. In the opposite limit of sparse grafting, $\gamma \ll 1$, the interactions between the side chains are relatively weak and manifest themselves only in the large-scale conformational properties of comblike macromolecule. We consider below both limits, $\gamma \gg 1$ and $\gamma \ll 1$.

We assume that the solution of comb−copolymer is dilute so that intermolecular interactions can be neglected as long as we focus on the single molecule conformational properties. The effects arising due to aggregation and phase separation in the solution are discussed separately.

3. Densely Grafted Copolymer, $\gamma \gg 1$

3.1. Free Energy and Θ Conditions for the Main Chain. We begin with the case $\gamma = n^{3/5}v^{1/5}/m^{1/2} \gg 1$. Here, the comblike copolymer acquires local cylindrical symmetry and can be considered as a polymer bottlebrush (an array of polymer chains end-grafted with axial separation h onto a long thin cylinder). Axial separation h characterizes the degree of extension of the backbone and is determined by the balance of the steric repulsion between crowded side chains and the entropic elasticity and the attraction between monomers of the backbone. The apparent contour length of comblike copolymer is $L = hM/m \leq M$ as long as the backbone is not completely extended, $h \leq m$. The backbone retains local flexibility on a length scale $\leq h$.

The free energy (per side chain) in the comblike copolymer can be represented as

$$F(D, h) = F^{(n)}(D, h) + F^{(m)}(h) \tag{2}$$

where

$$F^{(n)}(D, h) = F^{(n)}_{\text{conf}}(D, h) + F^{(n)}_{\text{int}}(D, h) \tag{3}$$

accounts for the free energy of a side chain ($F_{\text{conf}}{}^{(n)}(D, h)$ and $F_{\text{int}}{}^{(n)}(D, h)$ are entropy penalty due to extension of the side chain and the free energy of repulsion between the side chains, respectively), whereas $F^{(m)}(h)$ is the free energy of a spacer.

We remark that eq 2 contains only those contributions to the free energy of copolymer that scale linearly with overall molecular weight M, while lower order (in M) terms at this stage are neglected. This approximation is sufficient to analyze local conformational structure of the copolymer and to consider the conformational transitions induced by variations in solvent strength.

Following ref 5, we use the scaling model to examine local conformational structure of the comblike copolymer under poor solvent conditions for the backbone. The scaling model enables us to formulate the free energy of side chains (eq 2) with the account of local correlations of density fluctuations with the accuracy of numerical prefactors on the order of unity,

$$F^{(n)}_{\text{conf}}(D, h)/k_BT \cong \frac{D^2}{nc^{-1/4}v^{1/4}} \tag{4}$$

$$F^{(n)}_{\text{int}}(D, h)/k_BT \cong nc^{5/4}v^{3/4} \tag{5}$$

Here

$$c(D, h) \cong n/D^2h$$

is the average concentration (number density) of the side chain monomers within the distance D from the backbone. The free energy of the backbone $F^{(m)}_{\text{conf}}(h)$ depends on the solvent strength for the main chain and is specified below.

3.1.1. Extension of Side Chains. The equilibrium extension of the side chains $D = D(h)$ can be obtained by minimization of the free energy, eq 2, with respect to D and is given by[5]

$$D(h) \cong n^{3/4}h^{-1/4}v^{1/4} \tag{6}$$

The free energy of a bottle-brush with fixed axial separation h between the side chains yields

$$F^{(n)}(h) = F^{(n)}_{\text{conf}}(h) + F^{(n)}_{\text{int}}(h) \cong n^{3/8}h^{-5/8}v^{1/8} \qquad (7)$$

The backbone is subjected to axial tension induced by repulsion between the side chains. This axial tension is calculated as

$$f(h) = -\frac{\partial F(h)}{\partial h} \cong n^{3/8}h^{-13/8}v^{1/8} \qquad (8)$$

The radial polymer density profile as a function of distance r from the backbone is given by

$$c(r) \cong h^{2/3}v^{-1/3}r^{-2/3} \qquad (9)$$

with the cutoff at $r \cong D$.

3.1.2. Extension of Spacers: Θ Solvent Conditions for the Backbone. Under Θ solvent conditions for the main chain, $F^{(m)}(h) \cong h^2/m$. Here, the results of ref 5 are recovered. That is, the distance between neighboring side chains and the brush thickness are given respectively by

$$h_\theta \cong m^{8/21}n^{1/7}v^{1/21} \equiv m^{1/2}\gamma^{5/21} \qquad (10)$$

and

$$D_\theta \cong n^{3/5}v^{1/5}\gamma^{4/21} \qquad (11)$$

The free energy is given by

$$F_\theta/k_BT \cong \gamma^{10/21} \qquad (12)$$

whereas the axial tension yields

$$f_\theta/k_BT \cong F_\theta/h_\theta k_BT \simeq m^{-1/2}\gamma^{5/21} \qquad (13)$$

As has been discussed in ref 5, the extended spacers can be envisioned as strings of Pincus stretching blobs[10] of size

$$\xi_\theta \cong k_BT/f_\theta \cong m^{1/2}\gamma^{-5/21} \qquad (14)$$

Therefore, the spacer is extended with respect to its Gaussian dimension, $\xi_\theta \leq m^{1/2}$, provided that $\gamma \geq 1$. On a length scale smaller than ξ_θ, the backbone obeys the Gaussian statistics.

3.2. Poor Solvent Conditions for the Main Chain. 3.2.1. Onset of Collapse. According to the theory,[11] a linear polymer chain under poor solvent conditions acquires the globule conformation. The globule is characterized by the uniform polymer density τ and can be viewed as an array of densely packed thermal blobs of size $\xi_t \cong \tau^{-1}$. Inside the thermal blob the chain retains Gaussian statistics. The spherical shape of the globule is imposed by excess free energy of the globule−solvent interface arising due to unfavorable contacts of monomers with the solvent. The corresponding surface tension is $k_BT\xi_t^{-2}$.

As has been demonstrated earlier,[12] such a globule can be unfolded by applied external force. The unfolding transition occurs abruptly at $f \approx f_c$. The magnitude of the pulling force f necessary to transform the globule into a string of thermal blobs is $f_c/k_BT \cong \xi_t^{-1}$. When $f \ll f_c$, the spherical shape of the globule is only weakly perturbed. When $f \gg f_c$, the unfolded polymer chain exhibits the Gaussian elasticity (as long as the limit of total chain extension is not approached). Under the conditions when the end-to-end distance (larger than unperturbed globule size) is fixed, the spherical globule splits into an extended string of thermal blobs and a depleted globular bead. This coexistence occurs at constant (within the accuracy of the scaling model) tension f_c in the string of thermal blobs. Alternatively, a collapse of a linear polymer chain stretched by external force f occurs when $\tau \simeq \tau_c \cong f/k_BT$ or, equivalently, when size of the thermal blob in the collapsed state ξ_t becomes comparable to the size of the Pincus blob $\xi \cong k_BT/f$. When $\tau \geq \tau_c$ the globular bead appears as an undulation in the string of thermal blobs. An increase in τ leads to the growth of the bead due to "pulling in" the blobs from the strings. The distance between chain ends decreases in such a manner that at any value of $\tau \geq \tau_c$ the external force f is balanced by tension τ in the strings of thermal blobs.

For comblike copolymer with $\gamma \geq 1$, the axial tension arises due to the steric repulsion between crowded side chains. Therefore, the onset of collapse of the main chain occurs when the thermal blob size ξ_t becomes comparable to that of the Pincus stretching blob ξ_θ (eq 14), $\xi_t \simeq \xi_\Theta$. This condition determines the value of τ_c as

$$\tau_c \cong m^{-1/2}\gamma^{5/21} \qquad (15)$$

When $\tau < \tau_c$, the axial distance between side chains $h(\tau) \simeq h_\theta$. When $\tau \geq \tau_c$ the extension of the spacer $h(\tau)$ is determined from the condition $f(h)/k_BT \cong \tau$, where $f(h)$ is given by eq 8. Here, an increase in τ leads to a decrease in the spacer end-to-end distance h as

$$h(\tau) \cong n^{3/13}v^{1/13}\tau^{-8/13} \cong h_\theta\left(\frac{\tau_c}{\tau}\right)^{8/13}, \tau \geq \tau_c \qquad (16)$$

This result can be also obtained by minimization with respect to h of the free energy defined by eqs 2 and 7 with

$$F^{(m)}(h)/k_BT \cong \tau h + (m\tau^2 - \tau h)^{2/3} \qquad (17)$$

Here, the first and the second terms account for respective numbers of the thermal blobs in the strings and at the bead-solvent interface, where any h-independent contribution to the free energy of spacer is omitted.

Assuming that the local (axial) force balance holds at any grafting point (where the stretching force is applied to spacers), we find that when $\tau \geq \tau_c$ one globular bead appears in each spacer. These beads can move due to thermal fluctuations along the spacer and even coalesce with beads from neighboring spacers without changing the scaling dependence for $h(\tau)$, eq 16. Hence, in this regime the comblike copolymer retains the shape of a bottle-brush with weak longitudinal undulations in distribution of the main chain monomers. This regime and eq 16 hold when $\tau \geq \tau_c$. Upon further increase in τ, the number of thermal blobs at the bead-solvent interface exceeds that in the strings, and the second term in eq 17 dominates.

3.2.2. Necklace of Micelles. When $\tau \gg \tau_c$, the comblike macromolecule acquires the conformation of a necklace of intramolecular micelles connected by the strings of thermal blobs. (Each string comprises one or more spacers). The number of spacers forming the collapsed core of a micelle (equal to the number of side

chains forming the corona) is determined by the balance of the free energy of steric repulsion between the coronal chains with excess free energy of the core−solvent interface. In the framework of the scaling model, the aggregation number p, the thickness of the corona R_{corona} and the radius of the core R_{core} coincide with those for a starlike micelle[13,14] formed by diblock copolymer with the solvophilic block of degree of polymerization n and the solvophobic block of degree of polymerization m. The free energy per chain in such a micelle yields

$$F_{micelle}(p)/k_BT \cong (F_{corona}(p) + F_{interface}(p))/k_BT \cong p^{3/2} + (p\tau^2 m)^{2/3} \quad (18)$$

Equilibrium parameters of micelle are determined from the condition $d[F_{micelle}(p)/p]/dp = 0$ to give

$$p \cong (\tau^2 m)^{4/5} \quad (19)$$

and

$$F_{micelle}/k_BT \cong (\tau^2 m)^{6/5} \quad (20)$$

Corona thickness R_{corona} and core radius R_{core} are respectively given by

$$R_{corona} \cong n^{3/5} v^{1/5} p^{1/5} \cong n^{3/5} v^{1/5} (\tau^2 m)^{4/25} \quad (21)$$

and

$$R_{core} \cong (m/\tau)^{1/3p1/3} \cong m^{3/5} \tau^{1/5} \quad (22)$$

Remarkably $R_{corona}/R_{core} \sim \tau^{3/25}$ increases with inferior solvent strength, and the starlike shape of the micelle is preserved upon an increase in τ.

The interactions between intramolecular micelles determine the large scale conformation of the comblike copolymer. (For comparison, bridging attraction between intrachain micelles in polysoaps leads to the collapse of the long polysoap chain and eventually to the macrophase separation in the solution.[4]) For the comblike copolymer, the interactions between the intrachain micelles are governed by steric repulsion between the coronas. As has been demonstrated in ref 15, the repulsive potential arising in a confined corona of micelle is given by $U_{corona}(r)/k_BT \cong p^{3/2}\ln(R_{corona}/r)$, $r \leq R_{corona}$. In the framework of the scaling model the repulsive force acting between the micellar coronas can be estimated as $f_{corona}(r) \cong F_{corona}/R_{corona}$, $r \leq R_{corona}$. Therefore, $f_{corona}(R_{corona})/k_BT \cong (\tau^2 m)^{26/25}(n^3 v)^{-1/5} \cong \tau(\tau/\tau^*)^{27/25}$, where

$$\tau^* \cong (n^3 v)^{5/27} m^{-26/27} \cong m^{-1/2} \gamma^{25/27} \quad (23)$$

One can check that $f_{corona}(R_{corona})/\tau k_BT \geq 1$ when $\tau \geq \tau^*$. In other words, when $\tau \geq \tau^*$ the force of steric repulsion arising upon crowding between micellar coronas exceeds the tension in spacers, and therefore coronas are virtually nonoverlapped. On the contrary, when $\tau_c \leq \tau \leq \tau^*$ one expects significant overlap of the micellar coronas. (Note that $\tau_c \leq \tau^*$ when $\gamma \geq 1$.)

3.2.3. Overlapping Intrachain Micelles, $\tau_c \leq \tau \leq \tau^*$. When $\tau \leq \tau^*$, the repulsion between coronas of neighboring micelles is not sufficient to counterbalance the elastic tension in the strings of thermal blobs and to keep intramolecular micelles at the threshold of coronas overlap ($ph \simeq D$). Here, one expects strong interpenetration of the micellar coronas, and $D \gg ph$.

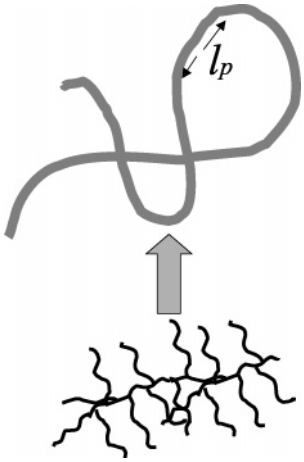

Figure 2. Schematic for comblike copolymer conformations.

Because of the axial confinement of the micellar coronas the bottle-brush formed by side chains preserves in general the axial symmetry despite significant density undulations of partially collapsed backbone. Hence, the free energy per coronal chain follows the scaling relation, eq 7, and is balanced by the surface free energy of the core, $F_{surface}/k_BT \cong p^{-1/3}(\tau^2 m)^{2/3}$. By using condition of the force balance for the backbone, $f(h)/k_BT \cong \tau$, where $f(h)$ is given by eq 8, we obtain aggregation number p in the confined (axially compressed) micelle:

$$p \cong \left(\frac{\tau}{\tau_{mic}}\right)^{37/13} \quad (24)$$

Here

$$\tau_{mic} \cong m^{-1/2} \gamma^{15/37} \quad (25)$$

Note that $\tau_c \ll \tau_{mic} \ll \tau^*$ when $\gamma \gg 1$. The intramolecular micelles start to appear when $p \geq 1$, or equivalently when $\tau \geq \tau_{mic}$. One can check that at $\tau \geq \tau_{mic}$ the second term in eq 17 dominates over the first term; i.e., the excess free energy of the bead interface is larger than the elastic free energy in the strings. This excess interfacial free energy drives the beads to aggregate into micelles when $\tau \geq \tau_{mic}$. Upon further increase in $\tau > \tau_{mic}$, the micellar corona becomes more symmetric,

$$\frac{D(h)}{ph} \cong \left(\frac{\tau^*}{\tau}\right)^{27/13} \quad (26)$$

Finally, when $\tau \cong \tau^*$ the regime of symmetric (nonconfined) spherical intramolecular micelles is recovered.

3.3. Coarse-Graining Approach and Separation of Length Scales. When $\gamma \gg 1$, the side chains are strongly overlapped, and the comblike copolymer is envisioned as a molecular bottle-brush. In this regime different characteristic length scales can be separated.

The *local conformational structure* of comblike copolymer (length scale $h < r < D$) is similar to that of a cylindrical brush with the elastic (intrinsically flexible) backbone. It is characterized by extension of both the side chains and the spacers.

We describe the conformation of a long comblike copolymer on a *larger scale* $r \gg D$ by using the coarse-graining approach (refs 5−8). In the framework of this model the comblike copolymer is envisioned as wormlike chain with an effective contour length $L \cong Mh/m$ and thickness D, Figure 2. As long as the spacers are not

completely extended, $h \ll m$, the effective contour length L is smaller than the bare contour length of the backbone M, $L \ll M$. The thickness D of the wormlike chain determines the lower cutoff length scale for this coarse-grained model. We recall that the backbone is locally flexible (the bare persistence length coincides with the monomer length a). The induced bending rigidity κ (arising due to increased repulsion between the side chains upon bending on length scale $\geq D$) gives rise to induced persistence length, $l_p \cong \kappa/k_BT$. If $l_p \geq D$, this persistence length manifests itself in large scale conformational properties (e.g., average end-to-end distance) of the macromolecule.

The two length scales are distinctly different, and the two persistence lengths, bare persistence length $\simeq a$ and induced persistence length $l_p \gg a$ are well-defined. On the length scale larger than l_p thermal fluctuations lead to bending of molecular bottle-brush axis. Long comblike copolymer with $L \gg l_p$ acquires a coiled conformation, while a shorter one with $L \leq l_p$ retains slightly perturbed cylindrical shape, Figure 2. Because of the steric repulsion between densely grafted side chains two segments of molecular bottle-brush do not interpenetrate each other. Therefore, the effective excluded volume for segment l_p of the bottle-brush is on the order of l_p^2D. For sufficiently long backbone, $L \gg l_p$, the comblike copolymer exhibits the self-avoiding walk (the swollen coil) conformation. Moreover, the repulsion between different macromolecules ensures aggregative stability of the solution with respect to macrophase separation.

When only short-range (excluded volume) interactions between the side chains are responsible for induced bending rigidity of a bottle-brush, the scaling argument give

$$l_p \cong D^2(h)F(h)/hkT = D^2(h)f(h)/kT \qquad (27)$$

where $F(h)/h$ is the free energy of bottle-brush per unit length, eq 7.

However, as has been discussed in refs 8 and 5, due to repartitioning of the side chains in a bent bottle-brush, the numerical factor in eq 27 is small, and the regime $l_p \gg D$ is reached only for sufficiently long and densely grafted chains. Earlier MC simulations of comblike copolymers[23] indicated $l_p \sim D$ (the lower cutoff limit for coarse-grained model). Recent self-consistent-field numerical calculations confirmed the existence of these two limits.[22]

Inferior solvent strength for the backbone leads to a decrease in the apparent contour length $L \cong Mh/m$ whereas induced persistence length l_p increases, eqs 27, 6, and 7. As a result, the overall size of the comblike copolymer

$$R \cong L^{3/5}l_p^{1/5}D^{1/5} \qquad (28)$$

varies with h as $R \sim h^{3/20}$ and only weakly decreases upon inferior solvent strength.

4. Sparsely Grafted Copolymers, $\gamma \ll 1$

In this section we consider the conformations of a sparsely grafted, $\gamma \ll 1$, copolymer under poor solvent conditions for the main chain.

4.1 Morphologies of Intramolecular Micelles. Weakly asymmetrical comblike copolymers with $\gamma \geq 1$ and $\gamma \leq 1$ form necklaces of starlike nonoverlapping spherical micelles at sufficiently low solvent quality for the main chain. On the contrary, strongly asymmetrical copolymers, $\gamma \ll 1$, are expected to form intramolecular aggregates in which the dimensions of solvophobic domain (formed by the spacers) exceed the size of solvophilic corona (formed by the side chains). These aggregates are reminiscent to the so-called crew-cut (CC) micelles of diblock copolymers.[16,18] Similar to the crew-cut micelles, the intramolecular aggregates can undergo morphological transformations in response to variations in solvent strength for solvophilic or solvophobic blocks. Three main morphologies for the intramolecular aggregates can be distinguished: (i) necklace of spherical micelles connected by extended spacers; (ii) unimolecular cylindrical wormlike micelle, in which the collapsed backbone forms the cylindrical core decorated by bottle-brush corona formed by the side chains; (iii) planar (lamellar) intramolecular aggregates of disklike shape, Figure 3. As we demonstrate below, for sparsely grafted copolymers with $\gamma \ll 1$, one can identify the regions of thermodynamic stability for all the three described morphologies. The conformational transitions between intramolecular aggregates of different morphologies can be triggered by inferior solvent strength for the main chain. Remarkably for densely grafted copolymers, $\gamma \geq 1$, only necklaces of starlike spherical micelles are found as equilibrium intramolecular aggregates.

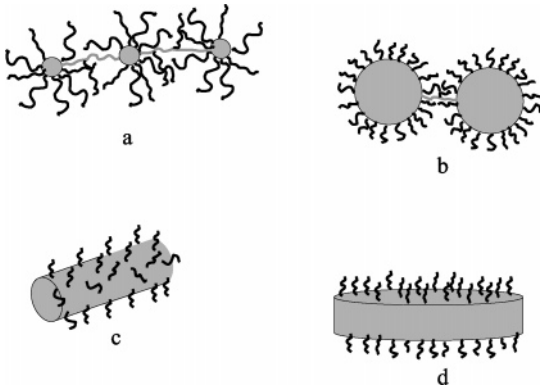

Figure 3. Morphologies of intramolecular micelles in amphiphilic graft copolymer: (a) necklace of starlike micelles; (b) necklace of spherical "crew-cut" micelles; (c) cylindrical wormlike micelle; (d) lamellar (disklike) structure.

To analyze the thermodynamic stability of different morphologies we formulate the free energy per side chain in aggregate of morphology i (i = 1, 2, 3 for lamella, cylindrical or spherical micelle, respectively) as

$$F^{(i)} = F^{(i)}_{corona} + F^{(i)}_{interface} + F^{(i)}_{core} \qquad (29)$$

where $F^{(i)}_{corona}$, $F^{(i)}_{interface}$, and $F^{(i)}_{core}$ are respective free energies of the corona (formed by solvophilic side chains), of the core−solvent interface and of the spacer in micellar core, respectively. We note that in the case of a necklace of spherical micelles, the free energy in eq 29 should be complemented by the contribution due to extended bridges connecting the spherical cores of micelles. However, at sufficiently high aggregation number $p \gg 1$, this contribution can be neglected. The second and the third terms in eq 29 can be respectively presented as $F^{(i)}_{interface}/k_BT \cong \tau^2 s^{(i)}(R)$ and $F^{(i)}_{core}/k_BT = b_iR^2/m$ where $s^{(i)}(R) = im/\tau R$ is the area per spacer at the core−solvent interface in aggregate of morphology i with core radius R, and $b_i = \{b_1, b_2, b_3\} = \{\pi^2/8, \pi^2/16,$

$3\pi^2/80\}$ are numerical coefficients calculated in ref 19. The first term in eq 29 can be presented with accuracy up to the second order in curvature terms as

$$F^{(i)}_{\text{corona}} \approx F^{(1)}_{\text{corona}}(1 - a_1^{(i)} D^{(1)}/R) \tag{30}$$

where

$$F^{(1)}_{\text{corona}}/k_{\text{B}}T \cong n v^{1/3} s^{-5/6}$$

and

$$D^{(1)} \cong n v^{1/3} s^{-1/3}$$

Here, $F^{(1)}_{\text{corona}}$ and $D^{(1)}$ are the free energy and the thickness of planar brush of side chains with grafting density $1/s(R)$, and

$$a_1^{(i)} = \frac{1}{2}\left(\frac{\partial \ln c^{(i)}(r)}{\partial \ln r}\right)_{\text{R}} - \frac{1}{2}\left(\frac{\partial(\ln f\{c^{(i)}(r)\})}{\partial(\ln r)}\right)_{\text{R}} \tag{31}$$

where $c^{(i)}(r)$ is radial polymer density profile in the corona and $f\{c^{(i)}(r)\}$ is the free energy per unit volume in the corona at distance r form the axis. Under good solvent conditions for coronal chains $f\{c^{(i)}(r)\} \sim \{c^{(i)}(r)\}^{9/4}$ (see ref 11). The scaling model envision the corona of micelle as an array of closely packed blobs, and the radial polymer density profile decays as $c^{(i)}(r) \sim r^{-2(i-1)/3}$, whereas the density of free energy decreases as $f\{c^{(i)}(r)\} \sim r^{-3(i-1)/2}$. Here, eq 31 gives $a_1{}^{(i)} = 5(i - 1)/12$.

Minimization of the two leading (at small curvatures) terms in eq 29, $F_{\text{corona}}{}^{(1)}(s) + F^{(i)}_{\text{interface}}(s)$, with respect to s gives the equilibrium surface area per spacer (or, equivalently, per side chain) at the core−solvent interface

$$s \cong \left(\frac{n v^{1/3}}{\tau^2}\right)^{6/11} \tag{32}$$

Correspondingly, the aggregation number p in the spherical micelle yields

$$p \cong (\tau m^{1/2} \gamma^{-15/7})^{14/11}$$

The average axial distance h between neighboring side chains in the cylindrical unimolecular micelle is given by

$$h \cong m^{1/2}(\tau m^{1/2} \gamma^{-20/13})^{-13/11} \tag{33}$$

We note that the dominant terms in the free energy of the intramolecular aggregate of morphology i are the same for all three morphologies. However, the linear in curvature correction to the free energy of corona is a decreasing (at constant s) function of i due to weaker crowding of the coronal chains in the sequence lamella − cylinder − sphere. On the contrary, the entropic penalty for extension of hydrophobic spacers in the core is an increasing (at constant s) function of i due to packing constraint. The binodal lines separating micelles of different morphologies are derived from the condition $F^{(i)} = F^{(i+1)}$ $(i = 1, 2)$ and are given by

$$\frac{\tau n^3 v}{m^2} \cong i(i+1)[b_{i+1}(i+1)^2 - b_i i^2] \tag{34}$$

Hence, the intramolecular morphological transformations of intramolecular aggregates occur at $\tau \cong \tau_{\text{morph}}$, where

$$\tau_{\text{morph}} \cong m^{-1/2} \gamma^{-5} \tag{35}$$

One can check that transformations $(i + 1) \rightarrow i$ (sphere-to-cylinder and cylinder-to-lamella transitions) occur upon a decrease in τ (or/and decrease in n or/and decrease in v_n or/and increase in m). On the contrary, an increase in τ (i.e., inferior solvent strength) leads to an increase in aggregation number in intrachain spherical micelles and to a progressive decrease in the ratio $R_{\text{core}}/R_{\text{corona}}$. The crossover $R_{\text{core}} \cong R_{\text{corona}}$ occurs at $\tau \cong \tau_{\text{cc}}$ where

$$\tau_{\text{cc}} \cong m^{-1/2} \gamma^{-25/3} \tag{36}$$

When $\tau \geq \tau_{\text{cc}}$ spherical intramolecular micelles are starlike, $R_{\text{core}} \leq R_{\text{corona}}$.

4.2. Aggregative Stability and Phase Separation. Despite a collapsed backbone in the cylindrical unimolecular micelle or in the necklace of spherical micelles, the copolymer solution remains stable with respect to macrophase separation. The reason for the solution stability is the local balance of the hydrophobic attraction between monomers of the main chain and of the steric repulsion between the side chains in the intramolecular aggregate. Further growth of hydrophobic domains (e.g., via intermolecular aggregation) is thermodynamically unfavorable. For spherical intramolecular micelles, the number of side chains (or spacers) per aggregate is the variable with respect to which system optimizes its structure. For a cylindrical unimolecular micelle, it is the number of side chains per unit length of the micelle. Both properties are optimized within a single chain aggregate. However, due to the long-range van der Waals attraction between condensed cores of lamellar disks the solution can undergo macrophase separation. As discussed in refs 16 and 17, whereas the van der Waals attraction between cylindrical micelles is insufficient to cause intermolecular aggregation, the lamellas do aggregate and precipitate in the sediment. Therefore, in the framework of the scaling model, the binodal (coexistence line) $\tau \cong \tau_{\text{morph}}$ separating the regions of stability of cylindrical and lamellar aggregates, coincides with the boundary of the two-phase region for copolymer solution. This boundary can be crossed upon an increase in the solvent strength for the solvophobic backbone. When $\tau \geq \tau_{\text{morph}}$, unimolecular micelles do not aggregate, and the solution remains homogeneous.

The collapse transition in a strongly asymmetrical comblike copolymer ($\gamma \ll 1$) occurs similarly to the coil-to-globule transition in a homopolymer in the vicinity of the Θ point. However, due to the presence of a small number of grafts (for which the solvent is good), the transition point (or, equivalently, the effective Θ temperature) is shifted with respect to the Θ temperature for the backbone. The detailed analysis of this transition incorporating the long-range intramolecular correlations is beyond the scope of our scaling model. To estimate the shift in the coil-to-globule transition temperature for comblike copolymer with respect to a homopolymer, we use a simple mean-field argument. In the framework of the mean-field model, superposition of attractive binary interactions between monomers of the backbone

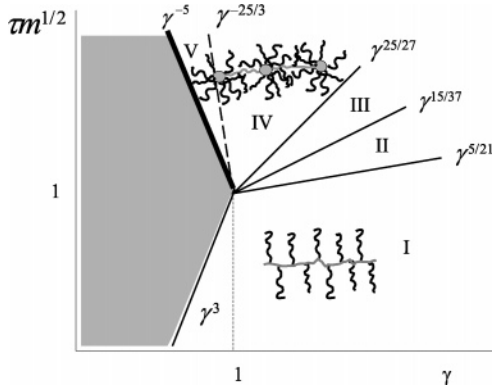

Figure 4. Diagram of states of the amphiphilic comblike copolymer in the (degree of branching, γ, reduced solvent strength, $\tau m^{1/2}$, coordinates). The regions of the diagram correspond to different conformations of the graft copolymer: (I) molecular bottle-brush with a stretched backbone; (II) pearl necklace with globular beads in the spacers; (III and IV) necklace of starlike micelles with overlapping (III) or nonoverlapping coronas (IV); (V) necklace of spherical crew-cut micelles. The bold line delineates the region of stability of unimolecular cylindrical micelle. The shaded region corresponds to the two-phase state of the solution.

(with the second virial coefficient $-\tau$) and repulsive interactions between the side chains (envisioned as swollen coils of size $\sim n^{3/5}v^{1/5}$ interacting via the second virial coefficient $\sim(n^{3/5}v^{1/5})^3$) leads to an effective (averaged) second virial coefficient of monomer−monomer interaction $v_{\text{eff}} \simeq (-\tau + m^{-1/2}\gamma^3)$. The effective second virial coefficient vanishes at $\tau = \tau_0 \cong m^{-1/2}\gamma^3$. Therefore, for an infinitely long sparsely grafted comb−copolymer, $\gamma \ll 1$

$$\tau_0 \cong m^{-1/2}\gamma^3 \tag{37}$$

determines the onset of the intramolecular collapse transition and of the corresponding phase separation in the solution.

5. Phase Diagram

The scaling phase diagram of states for comblike copolymer under poor solvent conditions for the main chain is presented in the ($\tau m^{1/2}$,γ) coordinates in Figure 4. Different regions in the diagram correspond to different conformations of the copolymer, the boundaries between the regions correspond to crossovers or to conformational transitions. The range $\tau \geq 0$ corresponds to poor solvent conditions for the main chain. The ranges $\gamma \geq 1$ and $\gamma \leq 1$ correspond to dense and sparse grafting of the side chains (overlapping or nonoverlapping under Θ solvent conditions for the backbone), respectively. When $\gamma \gg 1$, the intramolecular repulsion between the side chains induces the axial tension which prevents the collapse of the main chain as long as $\tau \leq \tau_c$, region I of the diagram. Further decrease in the solvent strength leads to partial (local) collapse of the main chain via formation of the pearl necklace structure. The pearls appear as globular beads in the extended spacers (when $\tau_c \leq \tau \leq \tau_{\text{mic}}$, region II). Subsequent coalescence of the beads results in formation of the intrachain starlike micelles. The aggregation number in the intramolecular micelle and the radius of the corona increase upon inferior solvent strength. The coronas of intrachain micelles are significantly overlapped (confined) in the range of $\tau_{\text{mic}} \leq \tau \leq \tau^*$, region III, or nonoverlapped (spherical) in the range of $\tau \geq \tau^*$, region IV. Remarkably, when $\gamma \geq 1$ only spherical starlike micelles with $R_{\text{core}} \leq R_{\text{corona}}$ are expected. Even weakly asymmetrical copolymers, $\gamma \leq 1$, form starlike intramolecular micelles as long as $\tau \geq \tau_{cc}$.

For strongly asymmetrical copolymers with $\gamma \ll 1$, a variety of morphologies for intramolecular aggregates are possible. Spherical starlike (region IV in the diagram) or crew-cut (region V) intramolecular micelles are formed under sufficiently poor solvent strength conditions (large τ), while intramolecular aggregates of other morphologies appear upon a decrease in τ. In the framework of the scaling model, the binodals for morphological sphere-to-cylinder and cylinder-to-lamella transitions (given by eq 34) coincide. They are marked in the diagram in Figure 4 by the bold line. Cylinder-to-lamella intramolecular transition leads to macrophase separation in the solution. The two-phase region is delineated by line $\tau = \tau_{\text{morph}}$ from above and by line $\tau = \tau_0$ from below. In the vicinity of $\tau \gtrsim \tau_{\text{morph}}$, the dilute phase contains comblike molecules with the backbone forming disklike planar lamella, whereas the sediment comprises the lamellar mesophase. In the vicinity of $\tau \geq \tau_0$, the dilute phase contains weakly collapsed spherical globules. When $\tau \leq \tau_0$, the solution is homogeneous. Here, the effective virial coefficient of monomer−monomer interaction is positive, and the comblike copolymer is slightly swollen.

6. Discussion and Conclusions

We have developed a scaling theory that describes the intramolecular conformational transitions in amphiphilic comblike copolymer induced by inferior solvent strength for the backbone. The model mimics the behavior of water-based copolymers (such as PNIPAM-*graft*-PEO, PNIPAM-*graft*-PAA or PPO-*graft*-PAA in high salt solution, etc.). The quality of water as a solvent for the so-called thermosensitive polymers (like PNIPAM or copolymer PEO/PPO) can be tuned by variations in temperature. Typically, the solubility of thermosensitive polymers in water decreases upon an increase in temperature.

Depending on grafting density of the side chains (or, the value of γ), two different scenarios of temperature-induced intramolecular conformational transitions are expected. Densely grafted comblike copolymer ($\gamma \gtrsim 1$) gives rise to the pearl necklace of spherical starlike intramolecular micelles. The solution of such pearl necklaces of micelles remains homogeneous. In the opposite case of weakly branched copolymer, $\gamma \lesssim 1$, necklaces of spherical micelles are supplemented by unimolecular aggregates of other morphologies (cylinder, lamella). Solutions of necklaces and unimolecular cylinders retain the thermodynamic aggregative stability. Transformation of cylinders into lamellar-like aggregates leads to macrophase separation in the solution.

Appearance of a pearl necklace of spherical micelles in densely ($\gamma \gg 1$) and moderately ($\gamma \simeq 1$) grafted copolymer is reminiscent to the pearl necklace formation in hydrophobic polyelectrolytes.[24] The latter is due to interplay of the short-range monomer−monomer attraction and the long range (in salt-free solution) Coulomb repulsion and is a manifestation of the Rayleigh instability[25] constrained by the chain connectivity. A necklace polyelectrolyte globule consists of globular beads connected by the strings of thermal blobs. The radius of a globular bead is governed by the balance of energy of the Coulomb repulsion between charged

monomers inside the bead and of excess free energy at the bead interface. The size of a bead turns out to be independent of solvent strength, while the number of monomers per bead increases $\sim\tau$ upon a decrease in solvent strength. As long as most of monomers associate in the beads, the number of beads per chain decreases with inferior solvent strength. The distance between neighboring beads (the length of a string) is determined by the balance of Coulomb repulsion between the beads and the elastic tension τ in the strings of thermal blobs. Therefore, the distance between neighboring beads increases $\sim \tau^{1/2}$ upon inferior solvent strength. Remarkably, screening of the Coulomb repulsion by added salt leads to coalescence of the beads when the screening (Debye) length drops down to the size of a bead.[26]

The physics of pearl necklace formation in comblike copolymer is similar to that in hydrophobic polyelectrolyte. In the case of comblike copolymer the same short-range attraction due to backbone monomers is counterbalanced by the steric repulsion between crowded side chains. The characteristic range for this repulsion is determined by dimensions of the side chains. The core of an intrachain micelle is an analogue of a globular bead in a polyelectrolyte necklace globule. The aggregation number (that is, the number of spacers involved in one intrachain micelle) is determined by balance of the steric repulsion in the corona and of the excess free energy at the core interface. Both the size and the number of monomers in collapsed core increase as a function of τ. The distance between neighboring micelles is determined by balance of the repulsion between coronas of the micelles and the tension in the strings of thermal blobs connecting the micelles. The equilibrium distance between micelles coincides with the span of micellar corona and increases with inferior solvent strength (the increase in τ).

Remarkably there is also a deep analogy between induced persistence length l_p that determines bending rigidity of a comblike copolymer, eq 27, and the electrostatic persistence length of a polyelectrolyte in a salt-added solution.[20,21] (The electrostatic persistence length is induced by the screened Coulomb repulsion between charged monomers.) In both cases, the origin of the long (though finite) range correlations along the chain is the repulsive interaction with a range exceeding monomer size a but still smaller than the overall macromolecule dimension. Equation 27 gives a correct scaling behavior for the electrostatic persistence length predicted by the OSF theory[20,21] if D is replaced by the Debye screening length and $F(h)/h$ is replaced by the electrostatic free energy per unit length of a charged line.

In contrast to densely branched ($\gamma \gg 1$) macromolecules, sparsely branched comblike copolymers ($\gamma \ll 1$) are more solvophobic. It is therefore not surprising that such copolymers can form intramolecular aggregates of diverse morphologies including pearl necklaces of spherical micelles, wormlike cylindrical micelles, and lamellar-like aggregates. The scaling theory predictions concerning polymorphism of the intramolecular aggregates are in qualitative agreement with recent computer simulations.[27] Clearly, the solubility of sparsely grafted comblike copolymer with hydrophobic backbone is limited. Two mechanisms of phase separation of the solution of such a copolymer are visible. At temperatures slightly below the Θ point for the backbone comblike copolymer collapses similarly to a homopolymer. That is, it forms a spherical globule with density slightly smaller than in a homopolymer globule due to weak repulsion between the sparse grafts. Aggregation of such globules leads to macrophase separation in the solution. On the contrary, at large values of τ an increase in solvent strength leads to morphological transformation of cylindrical unimolecular micelles into lamellar-like aggregates that associate due to the long-range van der Waals attraction (stacking interaction). Hence, there is an interval of temperatures τ where the solution of sparsely branched ($\gamma < 1$) comblike copolymer separates into dense sediment and dilute supernatant. We recall that the solution of densely branched copolymer ($\gamma > 1$) remains homogeneous at any τ values.

In conclusion, we emphasize the difference in the behavior of comblike copolymers with the same hydrophilic/hydrophobic balance but "inverted" topology. In contrast to stable solution of densely branched copolymer with collapsing backbone, the solution of polysoap undergoes macrophase separation. A long polysoap molecule with hydrophilic backbone and hydrophobic grafts collapses into a globule due to the bridging attraction. The globule comprises the hydrophobic domains of grafts surrounded by locally swollen coronas of the hydrophilic spacers. The same bridging attraction (that arises due to entropy gain upon exchange of the grafts between the hydrophobic domains in a single globule) leads to aggregation of the globules and macrophase separation of solution that occurs through transient network formation.

Acknowledgment. This work has been partially supported by EUROCORES program on Self-Organized Nanostructures (SONS) within the project 02-PE-JA016-SONS-AMPHI, Dutch National Science Foundation (NWO) program Computational approaches for multiscale modeling in self-organizing polymer and lipid systems No. 047.016.004, and by the Russian Foundation for Basic Research (Grant 02-03-33127).

References and Notes

(1) Halperin, A. Polymeric vs Monomeric Amphiphiles: Design Parameters. In *Supramolecular Polymers*; Ciferri, A., Ed.; Marcel Dekker, New York, 2000.
(2) Bohrisch, J.; Eisenbach, C. D.; Jaeger, W.; Mori, H.; Müller A. H. E.; Rehahn, M.; Schaller, C.; Traser, S.; Wittmeyer, P. *Adv. Polym. Sci.* **2004**, *165*, 1.
(3) Förster, S.; Abetz, V.; Müller A. H. E. *Adv. Polym. Sci.* **2004**, *166*, 173.
(4) (a) Borisov, O. V.; Halperin, A. Self-assembly of polysoaps. *Curr. Opin. Colloid Interface Sci.* **1998**, *3*, 415−421. (b) Collapsed and extended polysoaps. In *Associating polymers in aqueous media*; ACS Symposium Series 765; American Chemical Society: Washington, DC, 2000.
(5) Birshtein, T. M.; Borisov, O. V.; Zhulina, E. B.; Khokhlov, A. R.; Yurasova, T. A. *Polym. Sci. USSR* **1987**, *29*, 1293.
(6) Borisov, O. V.; Birshtein, T. M.; Zhulina, E. B. *Polym. Sci. USSR* **1987**, *29*, 1552.
(7) Rouault, Y.; Borisov, O. V. *Macromolecules* **1996**, *29*, 2605.
(8) Fredrickson, G. *Macromolecules* **1993**, *26*, 2825.
(9) Zhulina, E. B.; Vilgis, T. *Macromolecules* **1995**, *28*, 1008.
(10) Pincus, P. *Macromolecules* **1976**, *9*, 386.
(11) de Gennes, P. G. *Scaling Concepts in Polymer Physics*: Cornell University Press: Ithaca, NY, and London, 1979.
(12) Halperin, A.; Zhulina, E. B. *Europhys. Lett.* **1991**, *15*, 417.
(13) (a) Daoud, M.; Cotton, J.-P. *J. Phys. (Fr.)* **1982**, *43*, 531. (b) Birshtein, T. M.; Zhulina, E. B. *Polymer* **1984**, *25*, 1453.
(14) (a) Zhulina, E. B.; Birshtein, T. M. *Polym. Sci. USSR* **1985**, *27*, 570. (b) Halperin, A. *Macromolecules* **1987**, *20*, 2943.
(15) Witten, T. A.; Pincus, P. *Macromolecules* **1986**, *19*, 2509.
(16) Zhulina, E. B.; Adam, M.; LaRue, I.; Sheiko, S.; Rubinstein, M. *Macromolecules* Submitted for publication.

(17) Izzo, D.; Marques, C. M. *Macromolecules* **1997**, *30*, 6541.
(18) Borisov, O. V.; Zhulina, E. B. *Macromolecules* **2003**, *36*, 10029.
(19) Semenov, A. N. *Sov. Phys. JETP* **1985**, *61*, 733.
(20) Odijk, T. *J. Polym. Sci., Polym. Phys. Ed.* **1977**, *15*, 447.
(21) Skolnick, J.; Fixman, M. *Macromolecules* **1977**, *12*, 688.
(22) Feuz, L.; Leermakers, F. A. M.; Textor, M.; Borisov, O. V. Submitted for publication.
(23) Saariaho, M.; Ikkala, O.; Szleifer, I.; Erukhimovich, I. Ya., ten Brinke, G. *J. Chem. Phys.* **1997**, *107*, 3267.
(24) Dobrynin, A. V.; Rubinstein, M.; Obukhov, S. P. *Macromolecules* **1996**, *29*, 2974.
(25) Rayleigh, L. *Philos. Mag.* **1882**, *14*, 184.
(26) Borisov, O. V.; Hakem, F.; Vilgis, T. A.; Joanny, J.-F.; Johner, A. *Eur. Phys. J. E* **2001**, *6*, 37.
(27) Vasilevskaya, V. V.; Khalatur, P. G.; Khokhlov, A. R. *Macromolecules* **2003**, *36*, 10103.

MA047464S